Received: 24 November 2021 | Revised: 12 January 2022 | Accepted: 9 February 2022

DOI: 10.1111/jace.18411

Journal of the American Ceramic Society

RESEARCH ARTICLE

Theoretical estimation of dielectric loss of oxide glasses using nonequilibrium molecular dynamics simulations

Shingo Urata[1] | **Hiroyuki Hijiya**[2] | **Kazuhiko Niwano**[2] | **Jun Matsui**[3]

[1]Planning Division, AGC Inc., Tsurumi-ku Suehiro-cho 1-1, Yokohama, Kanagawa 230-0045, Japan

[2]Materials Integration Laboratories, AGC Inc., Yokohama, Kanagawa 230-0045, Japan

[3]Department of Physics, Faculty of Sciences, Kyushu University, Fukuoka, Fukuoka 819-0395, Japan

Correspondence
Shingo Urata, Planning Division, AGC Inc.
Email: shingo.urata@agc.com

Abstract

To theoretically explore amorphous materials with a sufficiently low dielectric loss, which are essential for next-generation communication devices, the applicability of a nonequilibrium molecular dynamics simulation employing an external alternating electric field was examined using alkaline silicate glass models. In this method, the dielectric loss is directly evaluated as the phase shift of the dipole moment from the applied electric field. This method enabled us to evaluate the dielectric loss in a wide frequency range from 1 GHz to 10 THz. It was observed that the dielectric loss reaches its maximum at a few THz. The simulation method was found to qualitatively reproduce the effects of alkaline content and alkaline type on the dielectric loss. Furthermore, it reasonably reproduced the effect of mixed alkalines on the dielectric loss, which was observed in our experiments on sodium and/or potassium silicate glasses. Alkaline mixing was thus found to reduce the dielectric loss.

KEYWORDS

dielectric loss, glass, mixed alkaline effect, molecular dynamics

1 | INTRODUCTION

The rapid increase in communication traffic due to the widespread use of the Internet of things, and machine-to-machine and device-to-device communication demands next-generation mobile communication technologies, such as 5G and 6G network systems.[1–5] Such advanced mobile communication systems require solutions for large-capacity transmission, low-latency transport, and ultradense cellular access. A key to increase the transmission capacity and data rate is expanding the communication bands to frequency ranges higher than the 380–5925 MHz range used in conventional network equipment.[1–3] The new band ranges from 6 to 60 GHz, and even higher ones up to 275 GHz would be applied in the coming technologies.[3]

A drawback of the high-frequency radio waves is their short connection range. Therefore, materials used for communication devices should aim to minimize traffic loss. In addition, it is necessary for even the architectural materials to be transparent for radio-wave applications because many devices are used indoors. It is thus important to know the dielectric loss of a variety of materials used to develop next-generation technologies.[6] In terms of glass substrates, considerable effort has been devoted to measure the dielectric loss at the GHz range for developing low-temperature Co-fired ceramics (LTCCs).[7] However, the glassy materials for LTCCs exhibit a low melting temperature and do not include alkalines; these materials are thus not suitable for window and cover glasses. Although Navias and Green reported the dielectric loss for over a hundred types of glasses,[8] data on glass compositions applicable to windows and cover glasses are very limited. Furthermore, most experimental data are limited in a narrow frequency range from 3 and 10 GHz, or even less than MHz range.[9–11] Therefore, theoretical method to

estimate dielectric loss of materials in a wide frequency range is necessary for efficiently exploring novel materials with a low traffic loss.

The dielectric loss of materials around the GHz, THz, and PHz ranges originates from the orientation, ionic, and electron polarizations, respectively.[12] As all the polarizations are related to the behaviors of atoms and electrons, quantum and classical molecular simulations are useful to theoretically evaluate the dielectric loss. For example, the dielectric property related to electron polarization is commonly calculated using *ab initio* calculations with density functional theory even for amorphous solids.[13,14] The orientation polarization of liquids of small molecules, such as water and methanol, has been widely investigated using classical molecular dynamics (MD) simulations[15–18] because the complex dielectric constant of a liquid can be evaluated from the autocorrelation function of the total dipole moment (**M**) based on the linear response theory developed by Kubo et al.[19] for dielectric relaxation as

$$\mathbf{M} = \sum_{i}^{N} \boldsymbol{\mu}_i, \tag{1}$$

$$\Phi(t) = \frac{< \mathbf{M}(t) \cdot \mathbf{M}(0) >}{< \mathbf{M}(0) \cdot \mathbf{M}(0) >}, \tag{2}$$

$$\frac{\epsilon^*(\omega) - \epsilon_\infty}{\epsilon_0 - \epsilon_\infty} = 1 - i\omega \int_0^\infty \Phi(t) e^{-i\omega t} dt, \tag{3}$$

where $\boldsymbol{\mu}_i$ is dipole moment of molecule i.

The equilibrium MD simulation method has been applied to polymers as well by defining the local dipole moment $\boldsymbol{\mu}$ at specific units composed of a polymer chain, allowing one to estimate the dielectric loss attributed to the orientation polarization of a polymeric solid.[20] In contrast, this method is not useful for inorganic amorphous materials such as an oxide glass, because there is no unique microstructure to define the local dipole moment $\boldsymbol{\mu}$. Thus, to measure the dielectric loss due to ionic polarization in an inorganic glass by MD simulations, another computational scheme is required. In this study, we develop a procedure to measure the dielectric loss of oxide glasses for a wide frequency range from 1 GHz to 10 THz by observing the response of the total dipole moment **M** to an applied alternating electric field using nonequilibrium MD simulations. To assess the accuracy of the proposed method, experimental measurements were also conducted focusing on the mixed alkali effect (MAE) on the dielectric loss. Note that MD simulations have been reported to be a useful method to investigate the MAE on glass properties.[21–26]

2 | COMPUTATIONAL AND EXPERIMENTAL METHODS

2.1 | MD simulations

All the glass models studied here were composed of approximately 20 000 atoms, and the side length of a cubic MD cell was approximately 6.5 nm. The model details are summarized in Table S1 of Supporting Information. In the initial configurations, atoms were randomly placed in a reticular pattern with an interval of 2.7 Å. Glass structures at 300 K and 0.1 MPa were obtained using the melt-quenching method,[27] in which the melted glass model at 3500 K for 500 ps was cooled down to 300 K at a cooling rate of 1 K/ps under an isobaric condition of 0.1 MPa with an isobaric-isothermal (NPT) ensemble.

After equilibrating the cooled glass model at 300 K for 500 ps, the following procedure was applied to measure the dielectric loss. Here, the MD simulations were switched from NPT to canonical ensemble (NVT).

1. The equilibrated model was converted to a slab model with the topped and bottomed free surfaces by eliminating the periodic boundary condition along a certain direction. The slab model has a vacuum layer with approximately 100 Å thickness, and the net volume was fixed.
2. The slab model was equilibrated at 300 K for 300 ps to relax the cutting surfaces.
3. An alternating electric field perpendicular to the glass surface was applied as, $\mathbf{E}(t) = A\sin(\omega t)$, where ω and A are the frequency and magnitude of the electric field, as shown in Figure 1(A). Note that A was set to 0.1 V/Å in this work, but lower amplitude is also useful for studying the MAE, as shown in Figure S1 of Supporting Information.
4. The overall dipole moment **M** of the glass model was defined as, $\mathbf{M} = \sum_{i=1}^{N} q_i \mathbf{r}_i(t)$, where N and $\mathbf{r}_i$ are the number of atoms in the glass model and the position of atom i, respectively. q_i is the partial charge on each atom i. In this work, the partial charge was set to be 60% of the ionic charge of each ion.
5. The real and imaginary parts of the complex dielectric constant were evaluated using the following definitions:

$$\mathbf{M}' = \epsilon' E = \frac{1}{t} \int_0^t \mathbf{M}(t') sin(\omega t') dt', \tag{4}$$

$$\mathbf{M}'' = \epsilon'' E = \frac{1}{t} \int_0^t \mathbf{M}(t') cos(\omega t') dt'.$$

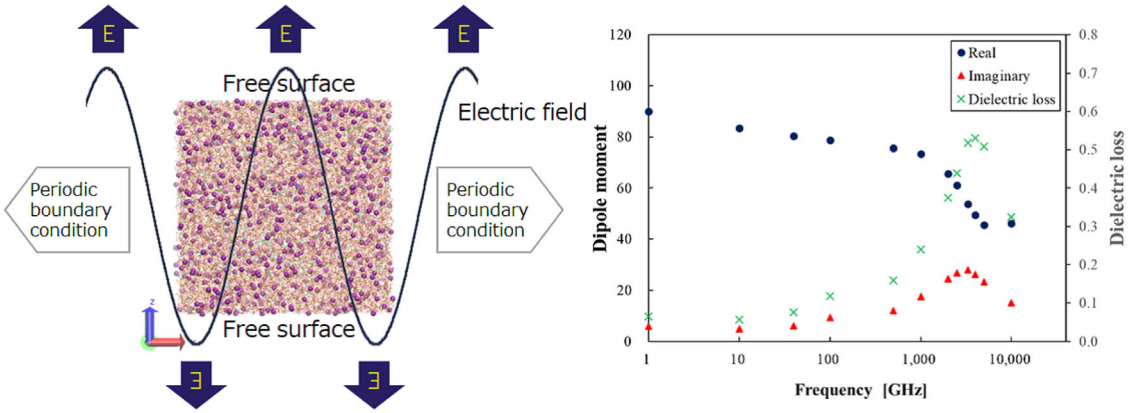

FIGURE 1 (Left) Schematic of nonequilibrium MD simulations with an external alternating electric field to measure dielectric loss. (Right) An example of frequency dependence of the real and imaginary parts of the dipole moment, and the dielectric loss evaluated using Equations (4) and (5)

6. Finally, the dielectric loss (tanδ) of the glass model was evaluated as

$$\tan\delta = \frac{M_z''}{M_z'} = \frac{\epsilon_z''}{\epsilon_z'}. \quad (5)$$

All the MD simulations were performed using the LAMMPS package.[28] An example of input file for the MD simulations with the alternating electric field is provided in the Supporting Information. The temperature and pressure were controlled using a Nosé–Hoover thermostat[29] and barostat.[30] The time step for integrating the atom motions was 1 fs. The interatomic potential proposed by Du et al. (namely, Teter potential)[31,32] was employed for all the simulations, because the force field is known to reproduce the MAE on resistivity.[26]

Using the nonequilibrium MD simulations, frequencies ranging from 1 GHz to 10 THz were examined. The simulation length t in Equation (4) depended on the frequency of the electric field applied, as summarized in Table S2 of Supporting Information. These values are based on the convergence of Equation (5) at 1 GHz for 12 cases, as shown in Figure S2 of Supporting Information. Practically, 50 periods are enough to converge the dielectric loss, which corresponds to 50 ns for 1 GHz, whereas a hundred periods were considered at frequencies higher than 40 GHz because the shorter simulation time allows us to obtain more data. To confirm the reproducibility of the theoretical calculations, all the three directions of a model were examined through simulations evaluating the frequency dependence of the dielectric loss, whereas two replicas obtained from different initial configurations were considered for investigating the MAE on the dielectric loss, implying that six simulations were conducted to obtain the average and deviations in dielectric loss.

2.2 | Experimental measurements

The glass samples experimentally investigated were $(SiO_2)_{77.3}(R_2O)_{22.7}$ (R = Na, K) and $(SiO_2)_{77.3}(Na_2O)_{11.35}(K_2O)_{11.35}$ glasses, which were identical to the substrates studied in [33], in which the topological origin of the MAE was identified. The glass samples were prepared from mixtures of reagent grade SiO_2, Na_2CO_3, and K_2CO_3 powders. After melted the ingredients at 1923 K in air, the melt was quenched and annealed at the glass transition temperature. Then, the glass samples were slowly cooled at 1 K/min cooling rate. The alkali ion contents were determined by a Z-2310 atomic absorption spectrophotometer (Hitachi High-tech Science Corp.) in aqueous solutions of the decomposed glasses. The analyzed glass compositions were shown in Table 1.

The procedure to prepare the glass samples is described in [33]. The dielectric loss of the alkaline silicate glasses was measured by a split post dielectric resonator (QWED)[34,35] at 10 GHz at room temperature. The software package 85071E option 300 (Keysight Technologies) was used for data analysis.

3 | SIMULATION RESULTS

3.1 | Response of the dipole moment to the electric field

First, responses of the dipole moment to the applied electric field were observed for 1 and 100 GHz and 5 and 10 THz using the glass model of $(SiO_2)_{80}(Na_2O)_{20}$ (Si80Na20), as shown in Figure S3 of Supporting Information. The dipole moment clearly followed the electric field. At frequencies of 1 and 100 GHz, there was no clear shift between the

TABLE 1 Experimentally measured glass compositions (mol%), density (g/cm^3), and dielectric loss at 10 GHz

Glass sample	SiO_2	Na_2O	K_2O	Density	ϵ'	Dielectric loss
$(SiO_2)_{77.3}(Na_2O)_{22.7}$	77.4	22.6	–	2.429	6.82	0.0222
$(SiO_2)_{77.3}(K_2O)_{22.7}$	78.3	–	21.7	2.439	7.03	0.0207
$(SiO_2)_{77.3}(Na_2O)_{11.36}(K_2O)_{11.36}$	77.3	11.5	11.2	2.404	6.57	0.0089

wave profiles of the dipole moment and the electric field, whereas there was a delay in the dipole moment from the electric field at 5 THz. This may be because the atoms in the glass model are unable to follow the electric field when a higher frequency is applied owing to friction acting on the moving ion with neighboring atoms.[36,37] These results imply that the dielectric loss of the glass model would increase with an increase in the frequency owing to the further delay in atomic motion. In contrast, the gap between the dipole moment and the electric field becomes smaller at a frequency of 10 THz compared to the case at 5 THz, as shown in Figure S3(d), indicating that the dielectric loss nonlinearly varies with an increase in frequency. The shorter ion displacement under higher frequency electric field may relate to the variation, but further detailed study is required.

As shown in Figure 1(B), the real and imaginary parts of the dipole moment along the direction of the electric field consistently vary over frequency, confirming that the proposed algorithm can capture the delay of the dipole moment of the amorphous glass model at a wide range of frequencies. The imaginary part of the dipole moment evaluated using Equation (4) increases with an increase in frequency up to 3.3 THz, it then begins to decrease in the case of the Si80Na20 glass. Consequently, the dielectric loss exhibits an evident peak at around 3.3 THz.

3.2 | Sodium silicates

Next, the effect of the alkaline content on the dielectric loss was examined using $(SiO_2)_{(100\text{-}x)}$ $(Na_2O)_x$ (x = 10, 20, 30, 40; Si$(100-x)$Nax) and amorphous silica glass (a-SiO_2) models, as shown in Figure 2. In the case of a-SiO_2, the dielectric loss did not increase considerably even at 10 THz, indicating that ionic polarization is very weak in glasses having no modifier cations. This result is qualitatively consistent with the experimental fact that the dielectric loss of a-SiO_2 is less than 0.001 in a wide frequency range from 100 Hz to 25 GHz,[7] although MD simulations tend to overestimate this dielectric loss.

In contrast, the sodium silicate glasses exhibited a larger dielectric loss compared to a-SiO_2, especially at frequencies higher than 100 GHz. With an increase in the Na_2O content, the dielectric loss increased and exhibited a higher peak in the THz region. According to these results, it is presumable that the displacement of sodium ions induced by the electric field is prevented by interaction with the glass network around the cations, and thus, the response of the dipole moment is delayed at the frequency range. The dielectric loss profiles of the sodium silicates generally decreased at a high frequency around 5 THz. This may be because the displacement of sodium ions is restricted within a short distance where the cations are insignificantly affected by the surrounding glass network under such a high-frequency electric field. The peak position shifts toward a higher frequency range with an increase in sodium content. A glass with a lower sodium content makes it difficult to create a continuous sodium diffusion pass, which may result in a lower dielectric loss at high frequencies.

In the low-frequency range (less than 100 GHz), the dielectric loss estimated by the nonequilibrium MD simulations was less than 0.1 for all the sodium silicate glasses. Navias et al. experimentally measured the dielectric loss of Si70Na30 at 3 and 10 GHz and reported it to be 0.019 and 0.024, respectively (Figure 2B).[8] The theoretical dielectric loss at these frequencies is approximately three times larger than the experimental data, indicating the overestimation tendency of MD simulations. One of the possible reasons for the discrepancy is the fixed charge of each ion with the Teter potential. To consider diffusive charge with classical MD simulations, a core–shell polarizable force-field[38] and a reactive force-field like ReaxFF[39] are useful; however, there lacks appropriate parameter sets to study the compositions with mixed alkaline. With an increase in sodium content up to 30 mol%, the dielectric loss increased, suggesting that a reduction in the alkaline content is effective at reducing the dielectric loss of glasses used for communication devices and architectures. This is also consistent with recent experimental measurements, which showed that the dielectric loss of alkaline silicates increased with an increase in alkaline content from 5 to 10 mol% at 10 GHz.[40]

3.3 | Effect of alkaline ion type

To understand the effect of the type of alkaline ion on the dielectric loss, $(SiO_2)_{80}(R_2O)_{20}$ {R=Li, Na, K} (Si80R20)

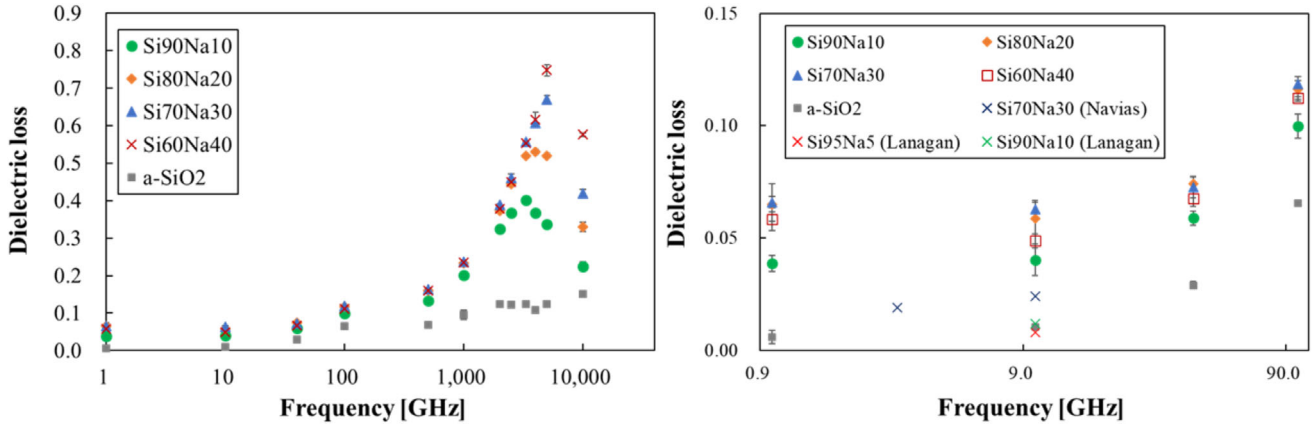

FIGURE 2 Dielectric loss theoretically estimated by MD simulations for the sodium silicate and amorphous silica glasses. The figure on the right shows an enlarged view on the results in the 1–100 GHz range, and the crosses represent the experimental data of Navias et al.[8] and Lanagan et al.[40] Error bars indicate the standard deviations of the dielectric loss obtained along the three directions

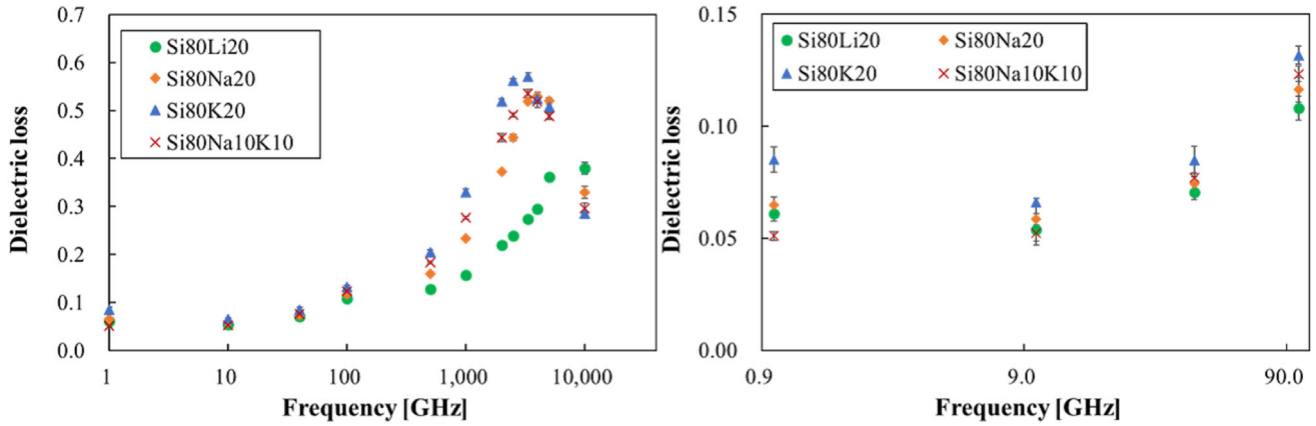

FIGURE 3 Dielectric loss theoretically estimated by MD simulations for $(SiO_2)_{80}(R_2O)_{20}$ {R=Li, Na, K} (Si80R20) glasses. The figure on the right shows an enlarged view for the results in the 1–100 GHz range. Error bars indicate the standard deviations of the dielectric loss obtained along the three directions

were compared, as shown in Figure 3. The dielectric loss of potassium silicate was found to be the largest followed by sodium silicate. The dielectric loss of lithium silicate was found to be the smallest. As the order of the dielectric loss is correlated to the ion radius, dielectric loss may be related to the difference in the ion mobility caused by the difference in the field strength of cations. This trend is also consistent with the experimental observations in [40], where the dielectric polarizability of alkaline silicate glasses with a full range of alkali species was investigated.

3.4 | Mixed alkali effect

Finally, the MAE on the dielectric loss was examined by comparing three glasses, $(SiO_2)_{80}(Na_2O)_{20}$ (Si80Na20), $(SiO_2)_{80}(K_2O)_{20}$ (Si80K20), and $(SiO_2)_{80}(Na_2O)_{10}(K_2O)_{10}$ (Si80Na10K10) using both experiments and MD simulations. Note that the glass compositions of the substrates that were experimentally measured were slightly different from the target ratios owing to evaporation that occurred during the melting process. According to Table 1, which summarizes the experimentally measured dielectric loss values at 10 GHz for the three glasses, the MAE on the dielectric loss was clearly observed. The lowest value was exhibited by Si80Na10K10.

Figure 4 compares the dielectric loss of the three glasses, theoretically calculated by the nonequilibrium MD simulations at 300 and 500 K. At 300 K, the MAE could be clearly observed at a frequency of 1 GHz as in the case of our experimental results, whereas the MAE could not be observed at frequencies higher than 10 GHz. The MAE related to ion diffusion is known to be caused by the different stable sites for different types of alkaline ions.[21–26] Because the migration length of alkaline ions is expected to reduce at higher frequencies, exchanges between the sites of alkaline ions

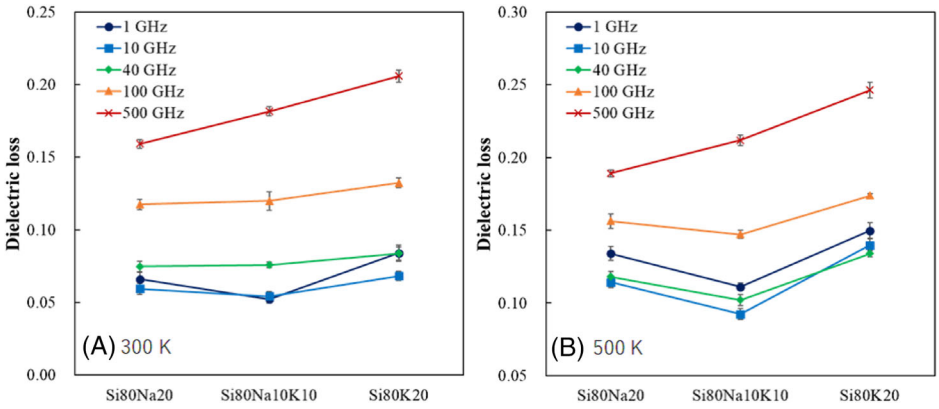

FIGURE 4 MD simulation results for effect of mixed alkalines on the dielectric loss of $(SiO_2)_{80}(Na_2O)_{10}(K_2O)_{10}$ (Si80Na10K10) glass compared to $(SiO_2)_{80}(Na_2O)_{20}$ (Si80Na20), $(SiO_2)_{80}(K_2O)_{20}$ (Si80K20) glasses. Error bars indicate the standard deviations of six simulations (two replicas and three directions)

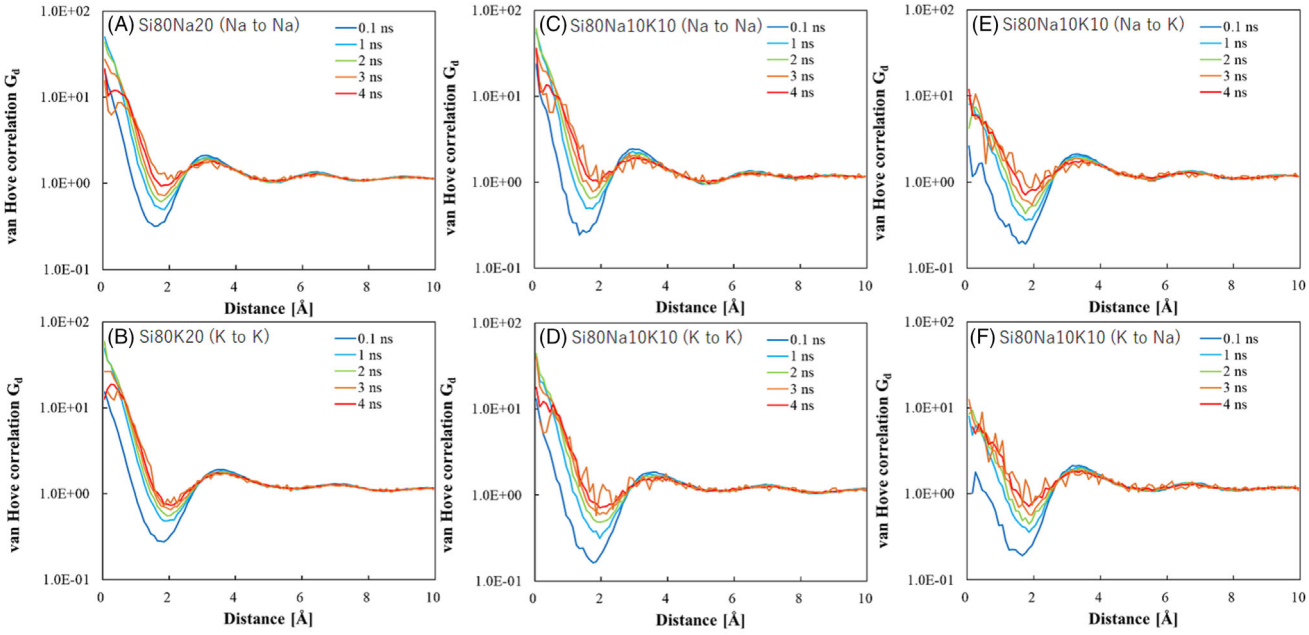

FIGURE 5 Distinct part of van Hove correlation functions at different MD simulation times for alkaline ions in the three glass models: (A) $(SiO_2)_{80}(Na_2O)_{20}$, (B) $(SiO_2)_{80}(K_2O)_{20}$, and (C)–(F) $(SiO_2)_{80}(Na_2O)_{10}(K_2O)_{10}$ (Si80Na10K10). (C) and (D) represent results for identical ions, and (E) and (F) show the results for sodium to potassium and potassium to sodium, respectively. All analyses were conducted for 5 ns MD trajectories for simulations with an external alternating electric field of 10 GHz at 500 K

would occur less frequently under a higher frequency electric field. Therefore, it would be reasonable that the MAE on the dielectric loss is more apparent at a lower frequency.

The MAE was also more obvious at a higher temperature of 500 K and was consistently observed up to 100 GHz, as shown in Figure 4(B). These results also indicate that the MAE on the dielectric loss occurs under more mobile conditions of alkaline ions. To confirm the relationship between the MAE and ion-site exchange frequency, the distinct van Hove correlation functions (G_d) were analyzed using the following equations and the 5 ns MD trajectories obtained with an alternating electric field of 10 GHz at 500 K, as shown in Figure 5.

$$G^i{}_d = \frac{N_\alpha + N_\alpha}{N_\alpha(N_\alpha - 1)} \left\langle \sum_{i=1}^{N_\alpha} \sum_{j=1}^{N_\alpha} \delta(r - |\mathbf{r}_i(0) - \mathbf{r}_j(t)|) \right\rangle, \quad (6)$$

$$G^d{}_d = \frac{N_A + N_B}{N_A N_B} \left\langle \sum_{i=1}^{N_A} \sum_{j=1}^{N_B} \delta(r - |\mathbf{r}_i(0) - \mathbf{r}_j(t)|) \right\rangle, \quad (7)$$

where N_α, N_A, and N_B are number of alkaline ions of each type, α, A, and B, respectively. The first equation is for the case of identical alkaline types, whereas the second one is

for distinct alkaline types, A and B.[26,41] The peak height at zero distance represents position exchange rate by the other atom. The peak height for the same ion types (Na to Na, and K to K) is higher than that for different ion types (Na to K, and K to Na), which indicates that the ion of the same type preferably takes over the site occupied by an ion. The results of the van Hove correlation analyses indicate that the exchange rate of positions between different alkaline ions is less than that between identical alkaline types, as in the case of [26], where the MAE on the resistivity of alkali aluminosilicate glasses was studied using MD simulations. Thus, alkaline mixing is an efficient way to decrease the dielectric loss of oxide glasses, and the origin of the MAE is the same as in the case of ion mobility at equilibrium conditions.

Note that MAE is observed more clearly when electric field of lower amplitude was applied, as shown in Figure S1 of Supporting Information. This phenomenon seems inconsistent with the effects of temperature and frequency of the electric field. Further detailed analysis is necessary to understand the origin of dielectric loss in the alkaline-containing oxide glasses as a subsequent study.

4 | CONCLUSIONS

To explore glass compositions applicable for next-gen communication devices by computational simulations, we proposed and validated a procedure to estimate dielectric loss of inorganic amorphous materials with employing a nonequilibrium MD simulation. In this method, an alternating electric field was applied to a glass model, and the dipole moment induced by the electric field was measured. According to the phase shift of the dipole moment from the applied electric filed, dielectric loss was successfully estimated in a wide frequency range from 1 GHz to 10 THz. Consequently, the MD simulations predicted that the dielectric loss of the alkaline silicate glasses reaches maximum at around a few THz range and then turns to decrease.

Comparing with several experimental data, it was found that the nonequilibrium MD simulation method reasonably reproduces effects of alkaline amount as well as the alkaline ion kinds on the dielectric loss, even though the theoretical calculation overestimates the dielectric loss to some extent. Interestingly, the MD simulation method could reproduce the mixed alkaline effect on the dielectric loss, which was experimentally observed by ourselves. These qualitative agreement between experiments and MD simulations confirmed that the proposed method is useful to evaluate the dielectric loss of novel amorphous materials instead of expensive experimental measurements.

Even though there is a further room to improve the simulation accuracy by investigating effects of model size, simulation time, forcefield, and so on, this work proved that the nonequilibrium MD simulation, which measures the dipole moment response to the alternating electric field, is a powerful tool for exploring low dielectric loss materials suitable for communication devices.

ORCID

Shingo Urata https://orcid.org/0000-0001-6878-345X

REFERENCES

1. Alliance N. 5G white paper. Next generation mobile networks, white paper, 2015;1.
2. Chen S, Zhao J. The requirements, challenges, and technologies for 5G of terrestrial mobile telecommunication. IEEE Commun Mag. 2014;52(5):36–43.
3. Osseiran A, Boccardi F, Braun V, Kusume K, Marsch P, Maternia M, et al. Scenarios for 5G mobile and wireless communications: the vision of the METIS project. IEEE Commun Mag. 2014;52(5):26–35.
4. Giordani M, Zorzi M. Satellite communication at millimeter waves: a key enabler of the 6G era. In: 2020 International Conference on Computing, Networking and Communications (ICNC). IEEE; 2020. p. 383-8.
5. Zhang L, Liang YC, Niyato D. 6G Visions: mobile ultra-broadband, super internet-of-things, and artificial intelligence. China Commun. 2019;16(8):1–14.
6. Muqaibel A, Safaai-Jazi A, Bayram A, Attiya A, Riad S. Ultrawideband through-the-wall propagation. IEE Proc Microw Antennas Propagation. 2005;152(6):581–8.
7. Sebastian MT, Jantunen H. Low loss dielectric materials for LTCC applications: a review. Int Mater Rev. 2008;53(2):57–90.
8. Navias L, Green F. Dielectric properties of glasses at ultra-high frequencies and their relation to composition. J Am Ceram Soc. 1946;29(10):267–76.
9. Thurnauer H, Badger A. Dielectric loss of glass at high frequencies. J Am Ceram Soc. 1940;23(1):9–12.
10. Rinehart D. Dielectric loss and the states of glass. J Am Ceram Soc. 1958;41(11):470–5.
11. Dutta A, Sinha T, Jena P, Adak S. Ac conductivity and dielectric relaxation in ionically conducting soda–lime–silicate glasses. J Non Cryst Solids. 2008;354(33):3952–7.
12. Kremer F. Dielectric spectroscopy–yesterday, today and tomorrow. J Non Cryst Solids. 2002;305(1–3):1–9.
13. Walker B, Dharmawardhana CC, Dari N, Rulis P, Ching WY. Electronic structure and optical properties of amorphous GeO2 in comparison to amorphous SiO2. J Non Cryst Solids. 2015;428:176–83.
14. Baral K, Adhikari P, Ching WY. Ab initio modeling of the electronic structures and physical properties of a-Si1- xGexO2 Glass (x= 0 to 1). J Am Ceram Soc. 2016;99(11):3677–84.
15. Neumann M. Dielectric relaxation in water. Computer simulations with the TIP4P potential. J Chem Phys. 1986;85(3):1567–80.
16. Anderson J, Ullo JJ, Yip S. Molecular dynamics simulation of dielectric properties of water. J Chem Phys. 1987;87(3):1726–32.

17. Skaf MS, Ladanyi BM. Molecular dynamics simulation of the wave vector-dependent static dielectric properties of methanol–water mixtures. J Chem Phys. 1995;102(16):6542–51.
18. Saiz L, Guardia E, Padró JÀ. Dielectric properties of liquid ethanol. A computer simulation study. J Chem Phys. 2000;113(7):2814–22.
19. Kubo R. Statistical-mechanical theory of irreversible processes. I. General theory and simple applications to magnetic and conduction problems. J Phys Soc Japan. 1957;12(6):570–86.
20. Matsui J, Hiwatari Y. Time autocorrelation function of intramolecular dipole moments for type-A polymer glass. J Phys Soc Japan. 2005;74(10):2849–52.
21. Habasaki J, Okada I, Hiwatari Y. MD study of the mixed alkali effect in a lithium&. zsbnd; potassium metasilicate glass. J Non Cryst Solids. 1995;183(1–2):12–21.
22. Habasaki J, Okada I, Hiwatari Y. MD study of the mixed alkali effect in terms of the potential surface in the lithium-potassium metasilicate glass. J Non Cryst Solids. 1996;208(1–2):181–90.
23. Habasaki J, Hiwatari Y. Molecular dynamics study of single and mixed alkali metasilicates-spatial and temporal characterization of the dynamics in the supercooled liquid and glassy states. J Non Cryst Solids. 2002;307:930–8.
24. Habasaki J, Hiwatari Y. Fast and slow dynamics in single and mixed alkali silicate glasses. J Non Cryst Solids. 2003;320(1-3):281-90.
25. Habasaki J, Ngai K, Hiwatari Y. "Cooperativity blockage" in the mixed alkali effect as revealed by molecular-dynamics simulations of alkali metasilicate glass. J Chem Phys. 2004;121(2):925-34.
26. Lodesani F, Menziani MC, Hijiya H, Takato Y, Urata S, Pedone A. Structural origins of the mixed alkali effect in alkali aluminosilicate glasses: molecular dynamics study and its assessment. Sci Rep. 2020;10(1):1–18.
27. Urata S, Sato Y. A study on the plasticity of soda-lime silica glass via molecular dynamics simulations. J Chem Phys. 2017;147(17):174501.
28. Plimpton S. Fast parallel algorithms for short-range molecular dynamics. J Comput Phys. 1995;117(1):1–19.
29. Nosé S. A unified formulation of the constant temperature molecular dynamics methods. J Chem Phys. 1984;81(1):511–9.
30. Tuckerman ME, Alejandre J, López-Rendón R, Jochim AL, Martyna GJ. A Liouville-operator derived measure-preserving integrator for molecular dynamics simulations in the isothermal–isobaric ensemble. J Phys A Math Gen. 2006;39(19):5629.
31. Du J, Cormack A. The medium range structure of sodium silicate glasses: a molecular dynamics simulation. J Non Cryst Solids. 2004;349:66–79.
32. Massobrio C, Du J, Bernasconi M, Salmon PS. Molecular dynamics simulations of disordered materials. Cham: Springer International Publishing; 2015.
33. Onodera Y, Takimoto Y, Hijiya H, Taniguchi T, Urata S, Inaba S, et al. Origin of the mixed alkali effect in silicate glass. NPG Asia Mater. 2019;11(1):1–11.
34. Krupka J, Geyer RG, Baker-Jarvis J, Ceremuga J. Measurements of the complex permittivity of microwave circuit board substrates using split dielectric resonator and reentrant cavity techniques. In: Seventh International Conference on Dielectric Materials, Measurements and Applications (Conf. Publ. No. 430). IET; 1996. p. 21–4.
35. Krupka J, Gregory A, Rochard O, Clarke R, Riddle B, Baker-Jarvis J. Uncertainty of complex permittivity measurements by split-post dielectric resonator technique. J Eur Ceram Soc. 2001;21(15):2673–6.
36. Boyd RH. Extension of Stokes' law for ionic motion to include the effect of dielectric relaxation. J Chem Phys. 1961;35(4):1281–3.
37. Zwanzig R. Dielectric friction on a moving ion. J Chem Phys. 1963;38(7):1603–5.
38. Dick Jr B, Overhauser A. Theory of the dielectric constants of alkali halide crystals. Phys Rev. 1958;112(1):90–103.
39. Van Duin AC, Dasgupta S, Lorant F, Goddard WA. ReaxFF: a reactive force field for hydrocarbons. J Phys Chem A. 2001;105(41):9396–409.
40. Lanagan MT, Cai L, Lamberson LA, Wu J, Streltsova E, Smith NJ. Dielectric polarizability of alkali and alkaline-earth modified silicate glasses at microwave frequency. Appl Phys Lett. 2020;116(22):222902.
41. Kob W, Andersen HC. Testing mode-coupling theory for a supercooled binary Lennard-Jones mixture I: the van Hove correlation function. Phys Rev E. 1995;51(5):4626.

SUPPORTING INFORMATION

Additional supporting information may be found in the online version of the article at the publisher's website.

How to cite this article: Urata S, Hijiya H, Niwano K, Matsui J. Theoretical estimation of dielectric loss of oxide glasses using nonequilibrium molecular dynamics simulations. J Am Ceram Soc. 2022;105:4200–4207. https://doi.org/10.1111/jace.18411